

# PROCEEDINGS OF SPIE

[SPIEDigitalLibrary.org/conference-proceedings-of-spie](https://SPIEDigitalLibrary.org/conference-proceedings-of-spie)

## Auto-labeling of respiratory time points in free-breathing thoracic dynamic MR image acquisitions for 4D image construction

Changjian Sun, Jayaram K. Udupa, Yubing Tong, Caiyun Wu, Shuxu Guo, et al.

Changjian Sun, Jayaram K. Udupa, Yubing Tong, Caiyun Wu, Shuxu Guo, Joseph M. McDonough, Drew A. Torigian, Robert M. Campbell, "Auto-labeling of respiratory time points in free-breathing thoracic dynamic MR image acquisitions for 4D image construction," Proc. SPIE 10953, Medical Imaging 2019: Biomedical Applications in Molecular, Structural, and Functional Imaging, 109531B (15 March 2019); doi: 10.1117/12.2513218

**SPIE.**

Event: SPIE Medical Imaging, 2019, San Diego, California, United States

# Auto-labeling of respiratory time points in free-breathing thoracic dynamic MR image acquisitions for 4D image construction

Changjian Sun<sup>1, 2‡</sup>, Jayaram K. Udupa<sup>2\*</sup>, Yubing Tong<sup>2‡</sup>, Caiyun Wu<sup>2</sup>, Shuxu Guo<sup>1</sup>, Joseph M. McDonough<sup>3</sup>,  
Drew A. Torigian<sup>2</sup>, Robert M. Campbell<sup>3</sup>

<sup>1</sup> College of Electronic Science and Engineering, Jilin University, Changchun, China.

<sup>2</sup> Medical Image Processing Group, 602 Goddard building, 3710 Hamilton Walk, Department of Radiology, University of Pennsylvania, Philadelphia, PA 19104, United States.

<sup>3</sup> Center for Thoracic Insufficiency Syndrome, Children's Hospital of Philadelphia, Philadelphia, PA, 19104, United States

## ABSTRACT

Determining the EE (End of Expiration) and EI (End of Inspiration) time points in the respiratory cycle is one key step during the 4D image construction from free-breathing dynamic thoracic computed tomography (CT) or magnetic resonance imaging (MRI) acquisitions. However, the cost of manually labeling EE and EI time points is extensive. An automatic image-based EE and EI labeling method makes image annotation independent of the image acquisition process, avoiding use of internal or external markers for the patient during image acquisition. The purpose of this paper is to introduce a novel optical-flow-based technique for finding EE and EI time points from dynamic thoracic MRI acquired during natural tidal-breathing. The diaphragm is tracked as a marker to determine the state of breathing. A region of interest (ROI) containing the diaphragm is selected to calculate the pixel optical flow values between two adjacent time slices. The average optical flow values of all pixels including diaphragm motion speed is used as a reference for labeling EE and EI. When the direction of movement of the diaphragm changes, EE or EI is found depending on the direction of the change. Quantitative evaluation was carried out to evaluate the effectiveness of our method in different locations in the lungs as compared to manual labeling. When tested on 28 patient dynamic thoracic MRI data sets, the average error was found to be less than 1 time point. Automatic labeling greatly shortened the labeling time, requiring less than 8 minutes compared to 4 hours for manual labeling per study.

## 1. INTRODUCTION

4D image construction of the thorax has been widely utilized in radiation therapy planning to quantify thoracic organ displacements, visualize abdominal and thoracic organ motion, and assess mechanical functions of organs [1, 2, 3]. Magnetic resonance imaging (MRI) is the modality of choice for imaging the pediatric thorax due to the absence of ionizing radiation, excellent soft tissue contrast, sufficient temporal resolution, and the ease of implementation of dynamic protocols [2]. The motivation and rationale for the presented work stem from the need to quantify dynamic thoracic function and its change due to surgical treatment in a pediatric ailment known as Thoracic Insufficiency Syndrome (TIS).

TIS is a complex condition involving malformation of the components of the thorax, mainly the rib cage, spine, sternum, and intercostal muscles [4, 5]. TIS patients often suffer from extreme deformities of the chest wall, diaphragm, and/or spine that prevent the chest from supporting normal breathing to cooperate with the requirements of imaging such as breath-holding or breathing cooperatively with a gating or tracking device. That is the reason that traditional 4D imaging methods cannot be implemented on TIS patients. To achieve 4D imaging under patient free-breathing conditions, a graph-based 4D MRI construction approach was proposed in previous work [2]. The method is purely-image based without the requirement of sorting based on a breathing signal or using any external surrogates.

Determining End of Expiration (EE) and End of Inspiration (EI) time points in the respiratory cycle from free-breathing slice acquisitions of the thorax is one key step needed for the above 4D image construction method via dynamic magnetic resonance imaging (dMRI) [2]. Considering the fact that typically, for each of 30-40 sagittal slice locations across the thorax, ~80 MRI slice data are acquired under free-breathing conditions over several respiratory cycles, the total number of resulting slices is ~2400 to 3200. Marking EE and EI points manually on all these slices is extremely labor-intensive and time-consuming. Previous work in this area performed this step manually [2] since current image-based methods cannot satisfactorily perform auto-labeling to facilitate 4D image reconstruction algorithms. This paper presents a novel optical-flow-based technique for auto-labeling of EE and EI points from MRI data acquired during unencumbered natural tidal-breathing. We expect this method to automate the labeling process with high accuracy and thereby shorten the overall 4D construction and analysis time for the TIS application.

## 2. MATERIALS AND METHODS

### *Image data*

Experiments are carried out on image data from Children's Hospital of Philadelphia (CHOP). This retrospective study was conducted following approval from the Institutional Review Board at CHOP along with a Health Insurance Portability and Accountability Act waiver. Image data sets utilized in our study all pertain to sagittal thoracic MRI. From right to left, each patient is scanned at 30-40 sagittal plane positions under breathing conditions that are natural for the patient. For each sagittal position, slice images are acquired at a rate of about 200-300 ms/slice over several breathing cycles, totaling 80 time points per sagittal location covering around 10 breathing cycles, which yields over 2000-3000 slices in total for one patient constituting a spatio-temporal sampling of the patient's dynamic thorax over 300-400 breathing cycles. The slices in our acquisition are  $224 \times 256$  pixels with a pixel size of  $0.78 \times 0.78 - 1.46 \times 1.46$  mm<sup>2</sup>. The 4D construction method we use [2] finds a small set of about 200-300 slices among these 2000-3000 slices to build one representative and optimal 4D image to describe the breathing motion of the 3D thorax in one respiratory cycle. The method, however, requires identifying which of the 80 time-point slices correspond to EE and EI time points for each sagittal location. Image data from a total of 28 patients were used in our experiment. The EE and EI time points for each data set were manually identified by a trained technician who has analyzed over 100 dMRI scans in this manner so far. These manual specifications provided the ground truth needed to test our auto-labeling method.

### *Main idea of auto-labeling*

The main idea of the method is to use the diaphragm indicated within a region of interest (ROI) as a surrogate to track upward and downward motion during the inspiration and expiration phases of the respiratory cycle. We use time-dependent optical flow computation to determine the direction and magnitude of the motion of the diaphragm. This vectorial motion (velocity) information is used to accurately determine the EE and EI time points for each sagittal location. In the labeling process, our method obtains its 79 velocity values from 80 time points by estimating the optical flow matrix within the ROI from the current and next time point. Finally, the EE and EI points are filtered by noting the points at which the direction of motion of the diaphragm changes from upward to downward (EE point) and downward to upward (EI point) direction.

### *ROI and Respiratory Surrogate*

In order to make our automatic labeling approach as consistent as possible with the ground truth labeling operation, we chose the diaphragm as a surrogate, since this is how manual labeling is done and the motion of each hemi-diaphragm contains maximal information about the respiratory cycle. To accurately track the movement of the diaphragm and reduce the effect due to deformation of other organs/tissues within the whole slice, we set an ROI roughly covering the superior dome of the diaphragm. The ROI is specified interactively by using the software CAVASS [6] as shown in Figure 1. The ROI needs to be specified manually only on the slice for one sagittal location per patient. The ROI is then propagated to all sagittal locations automatically.

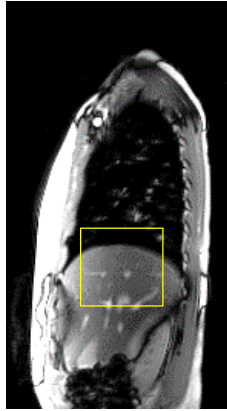


Figure 1. An ROI is selected interactively on one slice and determined automatically on all other slices of the dMRI acquisition.

### *Labeling EE and EI points by using optical flow*

An optical flow approach [7] is employed to automatically track the motion of the hemi-diaphragm in each lung (strictly speaking, the boundary that separates the base of the lung from the surrounding tissues) within the ROI. Since this motion tracking is done separately for each time sequence  $A_z = \{f_{T_1}, f_{T_2}, \dots, f_{T_M}\}$  (subscript  $z$  represents the sagittal position), we will describe the method for a single time sequence of slices. Figure 2 illustrates the main idea of the approach.

Consider a point such as  $P$  in the middle of the hemi-diaphragm dome. As the hemi-diaphragm in Figure 2(a) undergoes a complete inferior-superior-inferior (EI-EE-EI) motion during one breathing cycle,  $P$ 's  $y$ -location traverses a path. This is conceptually illustrated in Figure 2(b) where  $d_y(t)$  denotes this movement component of  $P$ . What is illustrated in Figures 2(a) and (b) is an ideal situation where  $t$  is assumed to be continuous (not discrete), and an individual point ( $P$ ) is tracked. In our practical set up, we can sample slices only at discrete time instances, which are indicated by small circles over one respiratory cycle in Figure 2(b). Instead of tracking individual points (pixels), we estimate an average of the motion of all points (pixels) in the vicinity of the hemi-diaphragm within the ROI by using the mechanism of optical flow estimated from each successive pair of adjacent time-slices  $f_{T_i}$  and  $f_{T_{i+1}}$  in  $A_z$ . The optical flow value we seek is a vector that denotes the velocity (speed and direction) of motion. The component  $v(t)$  of this vector in the  $y$  direction is illustrated in Figure 2(c).

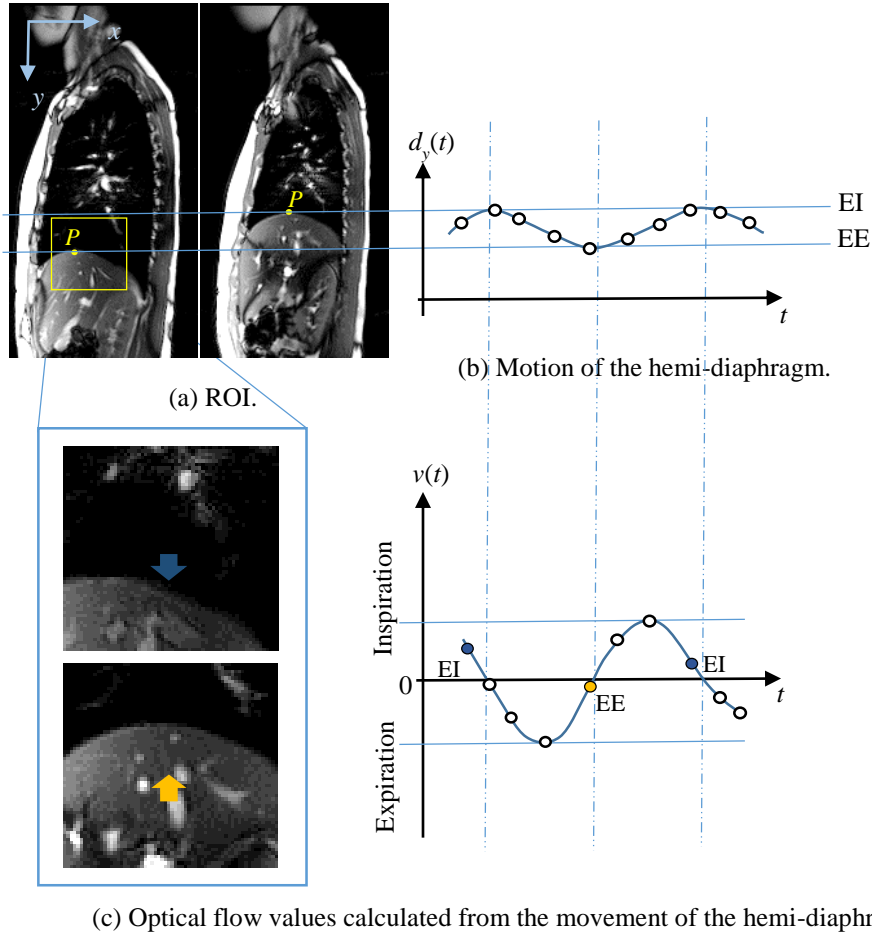


Figure 2. (a) A sample ROI. (b) The graph shows conceptually the continuous motion of the hemi-diaphragm over one respiratory cycle at point  $P$ . The small circles in (b) and (c) denote the sampled time-slices. (c) The vertical component  $v(t)$  of the velocity of the hemi-diaphragm at  $P$ . The detected EI and EE time points are marked in blue and orange, respectively.

Let  $V_z(p, t)$  denote the pixel image of the vertical component of velocity within the specified ROI at time  $t$  for the time sequence  $A_z$ . That is, at any pixel  $p$  within the ROI,  $V_z(p, t)$  denotes the velocity component  $v$  at pixel  $p = (x, y)$  at time  $t$  estimated via the optical flow method. To avoid undue influence of noise, instead of following motion at every pixel within the ROI, we estimate the average of the signed vertical velocity components within the ROI

$$\mu_z(t) = \frac{\sum_{p \in \text{ROI}} V_z(p, t)}{|\text{ROI}|} \quad (1)$$

where  $|\text{ROI}|$  denotes the number of pixels within the ROI. In short,  $\mu_z(t)$  is the average vertical velocity for slice location  $z$  at time  $t$ , with the convention that a +ve value of  $\mu_z(t)$  indicates downward motion of the hemi-diaphragm (inspiration) for  $z$  at time  $t$  and a -ve value denotes upward motion (expiration) for  $z$  at  $t$ .

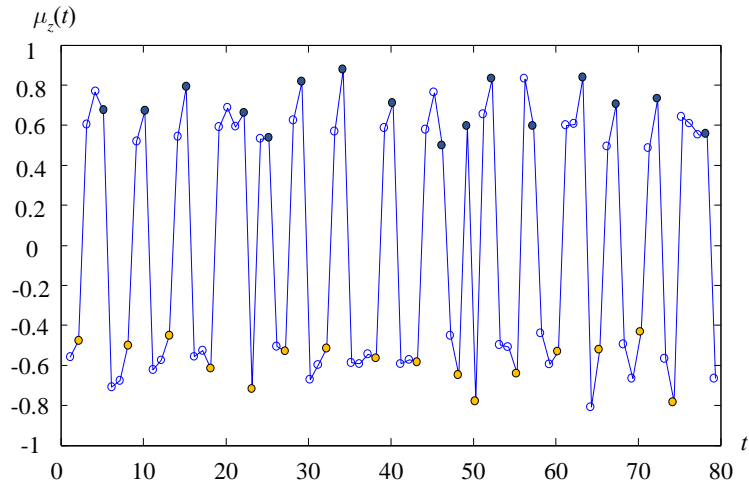


Figure 3. A plot of  $\mu_z(t)$  estimated from the time samples in  $A_z$  for a patient dMRI data set for a typical  $z$  location. The blue and orange dots denote EI and EE time points, respectively.

Figure 3 illustrates the variation of  $\mu_z(t)$  as a function of  $t$  as estimated by the above method in a time sequence  $A_z$  associated with a patient dMRI data set for the right hemi-diaphragm at a typical  $z$ -location. The pseudo-periodic motion of the hemi-diaphragm seems to be well-captured by the proposed technique. Recall that  $\mu_z(t)$  represents the vertical velocity of the hemi-diaphragm. During inspiration, the hemi-diaphragm moves caudally,  $\mu_z(t) > 0$ , and the EI time points are identified at time instances just before  $\mu_z(t)$  changes from a +ve (downward motion) to a -ve value (upward motion). Similarly, EE time points are estimated from  $\mu_z(t)$  at time instances just before  $\mu_z(t)$  changes from a -ve (upward motion) to a +ve value (downward motion). A complete respiratory cycle in Figure 3 extends from a colored time point to the next colored time point of the same color.

### 3. EXPERIMENTS AND RESULTS

#### *Accuracy of labeling*

Accuracy was quantified by estimating the deviation in the time instance determined by auto-labeling from the closest ground truth marking of the time points. To be specific, for a time sequence  $A_z = \{f_{T_1}, f_{T_2}, \dots, f_{T_M}\}$  associated with a  $z$ -slice, let an EE time slice determined by auto-labeling be  $f_{T_a}$  and the closest “true” time-slice be  $f_{T_i}$ . Then, the deviation in this instance is  $|t - a|$ . We estimated the mean  $\varepsilon_m$  (and standard deviation  $\varepsilon_{sd}$ ) of this error over the tested cases for EE and EI together (EE+EI), and separately for left lung (LL) and right lung (RL). Note that there were 28 4D dMRI acquisitions involved in our study, where each acquisition included 35-40 sagittal locations. Thus, our experiment involved 1,000-1,150 estimations where each estimation determined 2-4 time points for each of EE and EI. In other words, the total number of estimations of EE and EI time points in our experimental evaluation was  $\sim 65,000$ . The results are summarized in Table 1.

Table 1. Auto-labeling error (mean, SD) in terms of number of time points of deviation from manual labeling.			
	RL	LL	All
EE+EI	0.23 0.16	0.35 0.28	0.29 0.19

For some EE and EI points, it is even difficult for humans to distinguish respiratory status from slice acquisitions at two adjacent time points. The difference in lung motion is not significant between some adjacent time points. In our results we observed that the error in most locations is less than 1 time point slice. That is, in the sequence of 80 time point slices, some of which are labeled as EE and EI time points, the separation between ground truth labeling and auto-labeling is on the average off by less than 1 time point slice. This, we believe, is remarkable, considering that manual labeling can itself vary due to ambiguity by about that amount.

In the process of obtaining the optical flow value, the influence of other tissues in the background on the calculation is inevitable. The expansion and contraction of the heart will affect the labeling process, which can be shown by comparing errors of right and left lungs. The effect of heart motion on auto-labeling is more pronounced on the left side of the thorax. We observed that the accuracy of the RL at all locations is greater than the position corresponding to the LL, and the error of LL ( $0.35 \pm 0.28$ ) over all scenarios is higher than that of RL ( $0.23 \pm 0.16$ ). In addition, the background has a significant influence on the optical flow value, resulting in lower accuracy at edge areas of the lung. This effect can be verified from results at other locations.

#### *Computational time*

For MATLAB 2015a implementation on a Lenovo computer with 4-core, 3.7 GHz CPU (AMD A10-6700), 16GB RAM, and running the professional Windows 7 operating system, the human interaction time required per patient study for auto-labeling is at most 15 minutes. The actual purely computational time per study subsequently is ~8 minutes. In our experience of manually labeling all 28 dMRI data sets, a study typically takes about 4 hours for a trained technician. Thus, the auto-labeling method greatly facilitates analyzing a large number of TIS patient studies in a routine manner for studying the TIS phenomenon and its treatment outcomes.

## 4. CONCLUSIONS

In this paper, to make an image-based 4D construction approach efficient, we presented an optical flow based automatic annotation method for labeling EE and EI time points. The method tracks movement of the hemi-diaphragm to determine the breathing state by using optical flow. This method is independent of the image acquisition process without setting internal or external markers on the patient, allowing the patient to breathe freely, and without requiring gating or tracking devices. The auto-labeling process saves time greatly compared to manual labeling currently performed, which in turn makes the entire process of dMRI analysis for the study of TIS significantly more practical. Our extensive evaluation based on 28 dMRI data sets involving ~65,000 detection tasks suggests that the accuracy of the auto-labeling method to identify EE and EI phases is within 1 discrete time unit of temporal sampling. We conclude that the auto-labeling method performs at least as accurately as manual expert labeling and saves a considerable amount of human time needed in the process.

## 5. ACKNOWLEDGEMENTS

This research is supported by a “Frontier Grant” from The Children’s Hospital of Philadelphia and in part by the Institute for Translational Medicine and Therapeutics of the University of Pennsylvania through a grant by the National Center for Advancing Translational Sciences of the National Institutes of Health under award number UL1TR001878. The content is solely the responsibility of the authors and does not necessarily represent the official views of the National Institutes of Health. The training of Mr. Changjian Sun in the Medical Image Processing Group, Department of Radiology, University of Pennsylvania, Philadelphia, for the duration of two years is supported by the China Scholarship Council.

## REFERENCES

- [1] Tory, M., Röber, N., Möller, T., Celler, A., & Atkins, M. S. (2001). 4D Space-Time Techniques: A Medical Imaging Case Study. *Visualization, 2001. VIS '01. Proceedings* (pp.473-476). IEEE.
- [2] Tong, Y., Udupa, J. K., Ciesielski, K. C., Wu, C., McDonough, J. M., & Mong, D. A., et al. (2017). Retrospective 4D MR image construction from free-breathing slice acquisitions: a novel graph-based approach. *Medical Image Analysis, 35*, 345-359.
- [3] Cai, J., Chang, Z., Wang, Z., Paul, S. W., & Yin, F. F. (2011). Four-dimensional magnetic resonance imaging (4d-MRI) using image-based respiratory surrogate: a feasibility study. *Medical Physics, 38*(12), 6384-6394.
- [4] Campbell RM Jr, M. D., Mayes, T. C., Mangos, J. A., Willey-Courand, D. B., & Kose, N., et al. (2003). The characteristics of thoracic insufficiency syndrome associated with fused ribs and congenital scoliosis. *Journal of Bone & Joint Surgery American Volume, 85-A*(3), 399.
- [5] Campbell RM Jr, & Smith MD. (2007). Thoracic insufficiency syndrome and exotic scoliosis. *Journal of Bone and Joint Surgery-American Volume, 89 Suppl 1*(suppl 1), 108.
- [6] Grevera, G., Udupa, J., Odhner, D., Ying, Z., Souza, A., & Iwanaga, T., et al. (2007). CAVASS: A Computer-Assisted Visualization and Analysis Software System. *Medical Imaging 2007: PACS and Imaging Informatics*(Vol.6516, pp.51608-51608). International Society for Optics and Photonics.
- [7] Barron, J. L., Fleet, D. J., & Beauchemin, S. S. (1992). Performance of optical flow techniques. *Computer Vision and Pattern Recognition, 1992. Proceedings CVPR '92. 1992 IEEE Computer Society Conference on IEEE*(Vol.12, pp.236-242).